Catalytic Etching of {100}-oriented Diamond Coating with Fe, Co, Ni, and Pt Nanoparticles under Hydrogen

Tatsuya Ohashi, Wataru Sugimoto, Yoshio Takasu*

Department of Materials and Chemical Engineering,
Faculty of Textile Science and Technology, Shinshu University,
3-15-1 Tokida, Ueda, Nagano 386-8567, Japan
E-mail: ytakasu@shinshu-u.ac.jp (Y. Takasu)

Abstract

Etching of a highly {100}-oriented diamond coating, {100}HODC, with hydrogen gas using Fe, Co, Ni, and Pt nanoparticles as a catalyst was examined at high temperatures over 700°C by high-resolution scanning electron microscopy and Raman spectroscopy. The metal atoms vacuum-evaporated onto the {100}HODC formed nanoparticles themselves when heated at high temperatures; e.g. 700°C, in a flowing gas mixture of H_2 (10%) + N_2 (90%). At 800°C, short nano-channels and etch pits holding metal nanoparticles were formed by Fe, Co, and Ni. The shapes of the Co and Ni nanoparticles in the etch pits were affected by the shape of the etch pits; reversed pyramidal shape. On the other hand, the top view of the Fe nanoparticles embedded in the etch pits showed a distorted round shape, probably due to the formation of something such as iron carbide, while the carbon content was unknown. Apparently, etching of the {100}HODC by Pt nanoparticles was observed after the treatment at 1000°C. The difference in the catalytic etching behavior among these metal particles, the potential etching mechanism of diamonds with hydrogen by metal nanoparticles, probably as melted metal nanoparticles, and the formation mechanism of vacant etch pits were discussed.

Keywords: Oriented diamond coating, gasification, etching, etch pit, nano-channel, metal particle

---

*Corresponding author: Tel; +81 268 21 5455, Fax; +81 268 21 5452, E-mail address: ytakasu@shinshu-u.ac.jp (Y. Takasu)

1. Introduction

Carbon materials; such as carbon black, highly oriented pyrolytic graphite (HOPG), activated carbon, diamond crystallite, and boron-doped diamond (BDD), can be catalytically etched by hydrogen gas at high temperature with the help of various metal nanoparticles as a catalyst [1-7]. Nano-channels formed on BDD surface layers can be utilized to increase the applicability of BDDs [6, 7]. Nano-holes formed in activated carbon by etching, i.e., gasification, can be utilized for the increase of mesopores into the activated carbon to enhance the functionality of the porous carbon materials [4, 8-13]. The modification of the surface morphology of diamonds has been reported by many research groups [14-19], Jin el al. focused on the role of the molten rare-earth metals to etch away the diamond film surface [14, 15]. The oxidative etching using oxygen, oxygen/water vapor mixture gas and molten potassium nitrate, respectively have been reported [16]. For patterning of diamond, catalytic etching of diamond in the hydrogen atmosphere through thin solid metal film was studied [17]. On the other hand, fine patterning and selective etching of diamond by oxygen plasma etching through alumina or aluminum mask were demonstrated [18, 19]. The surface modification of synthetic diamond crystallites and BDDs with various metal nanoparticles and hydrogen has been reported only by our group [5-7]. The use of diamond crystallites and BDDs makes it possible to elucidate the relationship between the surface structure of diamonds and etching phenomena by metal nanoparticles. The cubic and hexagonal arrangements of carbon atoms on the {100} and {111} surfaces of diamond crystallites reflected on the shape of the etch pits; however, the rationale of the unique geometry of the etch pits and form of metal particles is still unclear.

In this study, the catalytic etching of Fe, Co, Ni, and Pt nanoparticles as a catalyst at a temperature between 700°C and 1000°C under a hydrogen atmosphere towards a highly {100}-oriented diamond coating, {100}HODC, was investigated. The flat surface of {100}HODC is profitable for the morphological investigation on the etching of the diamond surface by metal nanoparticles.

2. Materials and Methods

A highly {100}-oriented diamond coating, {100}HODC, formed on a Si(100) single crystal wafer using microwave plasma enhanced chemical vapor deposition [20], was

used in this study (provided by Kobe Steel, Ltd.). Vacuum evaporation method was applied to the loading of metal onto the {100}HODC, and the loading amount was monitored with a quartz thickness monitor (Anelva, EVM-32B). The specimen was placed in a Pt boat which was subsequently placed in a fused silica furnace tube and heated at a temperature between 700°C and 1000°C in a flowing gas mixture of H_2 (10%) + N_2 (90%) for a specified amount of time, typically 2 h. The specimen treated by this procedure was designated as *M*(*M*: Fe, Co, Ni, or Pt)-treated highly oriented diamond coating, i.e., *M*-{100}HODC. The structure of the specimens was characterized by high-resolution scanning electron microscopy (HR-SEM, Hitachi S-5000), Raman spectroscopy (Kaiser Optical Systems, Inc., Raman Microscope System 3000, YAG laser λ=532 nm) and X-ray diffraction (XRD, Rigaku RINT-2550 with monochromated CuK_α radiation at 40 kV and 40 mA). An XRD profile in the 2θ range of 20–95° was scanned at a scanning speed of 2° min^{-1}.

3. Results

3.1 Structure of the highly {100}-oriented diamond coating,{100} HODC

Figure 1 shows typical scanning electron microscopy (SEM) images of different magnifications of a pristine specimen of the {100}HODC used in this study. As pointed out with a white circle in Fig. 1-(b), the steps affected by epitaxial growth were found on the surface of the diamond; however, neither etch pits nor nano-channels could be observed on the surface. The X-ray diffraction (XRD) pattern of this diamond coating showed a strong peak from the (400) plane of the Si(100) single crystal wafer substrate, and a weak peak from the (111) plane of the {100}HODC. The {100}HODC was so thin that the peak could not be observed from the (400) plane of the {100}HODC on the XRD pattern in the experimental condition. The diffraction peaks from the (100) and (200) planes of the Si and the {100}HODC were not observed due to the extinction rule of the diamond structure.

[Fig. 1]

3.2 Etching of {100}HODC by Co nanoparticles in an hydrogen atmosphere

Usually, the metal atoms deposited on flat and dense substrates by vacuum evaporation cohere, resulting in small metal particles being dispersed on the substrate. Figure 2-(a) shows an SEM image of a Co-{100}HODC treated at 700°C for 2 h, in which the deposited amount of Co was 5.0×10^{15} Co-atoms cm^{-2}. The round small particles on the SEM image were confirmed as Co particles by back-scattering SEM. Thus, many Co nanoparticles with less than ca. 20 nm in diameter were formed on the {100}HODC after the heat-treatment at 700°C; however, there is no evidence of etching of the {100}HODC by the Co nanoparticles in either the secondary or the back-scattering SEM images for this specimen.

[Fig. 2]

Upon heating of the Co-deposited specimen at 800°C under a hydrogen atmosphere for 2 h (Fig. 2-(b)), the Co particles not only cohered but also acted as a catalyst for the gasification of diamond with hydrogen gas. In a previous report concerning the etching of the surface layers of a synthetic diamond powder with Co nanoparticles, methane was detected as a product of the gasification by hydrogen, and both nano-channels and etch pits on the {111} planes, as well as etch pits on the {100} planes, were observed [2]. The SEM image in Fig. 2-(b) shows that some Co nanoparticles exist at the holes created by themselves (indicated with a white square), while others exist at the end of short nano-channels (indicated with a white circle). Since few Co nanoparticles are observed just around the larger Co nanoparticles embedded in the etch pits and nano-channels, the larger Co nanoparticles may be formed by incorporating the small Co particles near the Co nanoparticles. The top view of the Co nanoparticles in Fig. 2-(b) shows a square with round corners rather than a circle (see the enlarged SEM image inserted in the left upper part of the figure). Although the spherical shape of Co nanoparticles is usually stable at high temperatures due to the high cohesion energy of Co, the Co nanoparticles shown in these images must be formed by the restriction caused by the shapes of the etch pits, presumably a reversed pyramidal shape with four {111} planes of the diamond. The flatness of the walls of the etch pits strongly suggests that the {100}HODC was etched by Co nanoparticles being restricted by the

arrangement of the carbon atoms of the {111} planes of the diamond structure.

As shown in the SEM images of the Co-{100}HODC treated at 900 °C for 2 h (Fig. 2-(c)), the results of the etched surface of the {100}HODC were almost the same as those of the Co-{100}HODC treated at 800°C for 2 h; however, vacant etch pits, i.e., etch pits embedding no Co nanoparticles, were also observed (indicated with a white triangle). The formation of the vacant etch pits will be discussed in the discussion section.

3.3 Etching of {100}HODC by Ni nanoparticles

~~Figures 8, 9, and 10~~ Figure 3 shows the results of etching for Ni-{100}HODC (in which the deposited amount of Ni was 5.0×10^{15} Ni-atoms cm^{-2}) treated at 800°C, (a), and 900°C, (b). No evident difference in the conditions of the shapes of Ni nanoparticles; short nano-channels and etch pits, was observed on these SEM images relative to those of Co-{100}HODC. Heating for a longer time, i.e., 24 h, in a hydrogen atmosphere at 900 °C, (c), as presented in Fig. 3-(c), increased the extent of etching and resulted in the formation of many etch pits with and without Ni nanoparticles (indicated with a white triangle). Even a large etch pit of about 100 nm in diagonal length was formed in the surface layers of the specimen (indicated with a white circle).

[Fig. 3]

3.4 Etching of {100}HODC by Fe nanoparticles

Figure 4-(a) shows an SEM image of Fe-{100}HODC treated at 800°C for 2 h, in which the deposited amount of Fe was 5.3×10^{15} Fe-atoms cm^{-2}. Many distorted round forms of Fe nanoparticles, which appeared to be bulging out from their respective etch pit sites, are observed on the terrace of the {100}HODC, although neither nano-channels nor etch pits were seen except near the edge part. Upon heating at 900°C for 2 h, as shown in the SEM image of Fig. 4-(b), the Fe-{100}HODC had many vacant etch pits with flat walls (indicated with white triangles) on the surface in addition to the distorted round forms of Fe nanoparticles. The formation of distorted round-shaped Fe nanoparticles probably related to the formation of something such as “iron carbide”, while the carbon content is unknown, because the solubility of carbon into iron is much higher than that into Co, Ni, and Pt [21]. Differently from the case of the Co, Ni, and Pt

nanoparticles, the “iron carbide” particles may not easily form round-shaped particles even at 900°C, and they also bulged the etch pits probably due to the incorporation of both carbon, from the diamond, and ion particles surrounding them. It is still uncertain whether any iron-related particles exist in the apparently vacant etch pits or any small “iron carbide” particles exist in them.

[Fig. 4]

3.5 Etching of {100}HODC by Pt nanoparticles

Figure 5 shows SEM images of Pt-{100}HODCs (in which the deposited amount of Pt was 1.5×10^{15} Pt-atoms cm^{-2}) treated at (a); 900°C and (b); 1000°C, for 2 h, respectively. The size of the Pt nanoparticles formed on the Pt-{100}HODC treated even at 1000°C was smaller than about 8 nm in diameter. By treatment of the Pt-{100}HODCs at 900°C, the finely dispersed platinum nanoparticles were observed, and neither etch pits nor nano-channels was apparently found on the {100}HODC; however, many etch pits were observed for the specimen treated at 900°C, where much more amount of Pt was loaded on synthetic diamond crystallites [22]. On the SEM images of the specimen heat-treated at 1000°C, many etch pits were clearly observed (Fig. 5-(b)). Although it is well known that the size of metal particles drastically increased with increasing heat treatment temperature [2], the SEM images suggested that the aggregation of the nanoparticles were controlled being restricted by the walls of the etch pits. The temperature needed for the formation of etch pits by Pt nanoparticles was higher than that required by Fe, Co, and Ni nanoparticles. Such a difference may be caused by both the difference in the size and the melting point of the metal nanoparticles. As shown in Fig. 5-(b), two types of etch pits formed on the surface of the Pt-{100}HODC: the first one holds a Pt nanoparticle (indicated with a circle), and the second one holds no Pt nanoparticle (indicated with a white triangle).

The specific etching behavior of {100}HODC with various metal nanoparticles described above is summarized in Table 1.

[Fig. 5]

[Fig. 6]

[Table 1]

3.6 Raman spectroscopy for the pristine {100}HODC and M-{100}HODCs

Figure 18 shows the Raman spectra of the Fe-{100}HODC, Co-{100}HODC and Ni-{100}HODC treated at 900°C for 2 h and that of a pristine {100}HODC. For each specimen, D and G peaks, which lay at ca. 1334 and 1540 cm^{-1}, respectively, were observed, while the pristine {100}HOCD gave a peak at 1509 cm^{-1} in the wave number region between 1400 and 1650 cm^{-1}. The band at 1334 cm^{-1} is assigned to the sp^3-bonded carbon in diamond (D band) and reflects the highly crystallized nature of the deposited film [23]. The broad peak around 1540 cm^{-1} is attributed to the sp^2-bonded carbon (G band) [24]. The peak intensity ratio of the D band to the G band (I_D/I_G) is a measure of the amount of graphitic impurities. The measured I_D/I_G values, where I_G was the spectrum intensity at 1540 cm^{-1} even for the pristine {100}HODC, of the Fe-{100}HODC, Co-{100}HODC, Ni-{100}HODC and pristine {100}HODC were 0.56, 0.59, 0.47 and 0.29, respectively, with no obvious dependence on the metal species. The result suggests that the diamond structure was maintained after the catalytic etching by metal nanoparticles. The higher I_D/I_G values of the *M*-{100}HODCs than that of the pristine {100}HODC suggest that the sp^2-bonded carbon impurities that had been formed on the pristine {100}HODC was partially removed by the metal particles through the etching of the surface layers of the {100}HODC.

4. Discussion

4.1 Formation of vacant etch pits by metal nanoparticles

The {100}-oriented diamond coatings were patterned with Fe, Co, Ni, and Pt nanoparticles for the catalytic etching at temperatures over 800°C in a hydrogen atmosphere. The formation of vacant etch pits observed for these four kinds of *M*-{100}HODCs strongly suggests that the respective metal nanoparticles slipped out the etch pits walled with four {111} planes of the diamond. As the reasons for the metal nanoparticles to be able to slip out the etch pits of the {100}HODCs, the following ones

should be pointed out: (1) the treatment temperature of the *M*-{100}HODC was very high, i.e., higher than 900°C; (2) since the melting point of a metal nanoparticle generally decreases with a decrease in the particle size; for example, the melting point of bulk gold is ca. 1300 K and that of ultrafine gold particle with 2 nm in mean diameter was reported as about 600 K [25], the metal nanoparticles investigated in this study must reach the melted state at temperatures higher than 900°C; (3) since the {111} planes of diamond is the closest packing plane, metal nanoparticles can move on the flat surface of the {111} planes more easily than on the {100} plane; (4) since the surface carbon atoms of the {111} planes of diamond have no dangling bond, they must be less active than those of the {100} plane which have dangling bond. These four factors must enable the melted metal nanoparticles to slip out of the etch pit before the metal particle becomes too large in the etch pit.

4.2 Potential etching mechanism of {100}HODC with H_2 and metal nanoparticles

Concerning the etching behavior of diamonds with hydrogen and metal nanoparticles, the following information has already been obtained by our group [5-7]: (1) heating of diamonds (diamond powder, BDD, and {100}HODC) on which metal particles (Fe, Co, Ni, Ru, Nb, Mo, W, and Pt) are loaded in a flowing gas mixture of H_2 (10%) + N_2 (90%) at 1 atm at temperatures higher than 800°C introduced nano-holes (etch pits) and/or nano-channels into the surface layers of the diamonds; (2) methane was detected during etching of the diamonds under a hydrogen atmosphere; (3) nano-channels are preferentially formed on the closest packing plane of {100} of the diamonds, while etch pits are rarely formed; on the other hand, etch pits walled with four {111} planes, presumably a reverse pyramidal shape, are formed on the {100} planes of the diamonds; (4) both the bottom and the walls of the nano-channels are flat; (5) similar to diamond, other carbon materials, such as graphite [2, 3], carbon black [1], and activated carbon [4], are also etched with hydrogen by metal nanoparticles as the catalysts.

The flatness of the walls of the etch pits and the bottoms of the nano-channels strongly suggests that diamonds were etched by the melted metal nanoparticles. The formation of methane signifies that the surface carbon atoms of the diamond react with hydrogen with the help of the metal nanoparticles as catalyst. The melted metal nanoparticles absorb carbon atoms more easily than solid metal nanoparticles up to the

limit of the solubility. One method for the synthesis of carbon nanotubes requires the use of a gas mixture of methane, hydrogen, and inert gas at high temperature [26-28]. In the case of the etching of diamonds in this study, the pressure of hydrogen was very high (0.1 atm), and that of methane was very low because the gaseous product (methane) on the diamond was promptly blown away by the flowing gas mixture of H_2 and N_2. Thus, etching of diamond must proceed through something similar to a reverse reaction of the formation of carbon nanotubes; i.e., the absorbed or adsorbed carbon atoms on the metal nanoparticles react with hydrogen, resulting in the formation of methane. Since taking of the carbon atoms from diamonds by the metal nanoparticles occurs from the weakly bonded atoms of diamond, the carbon atoms of the closest packing plane of diamond, which have no dangling bond, are the most stable against the taking out of the carbon by metal nanoparticles, as compared to the other crystal planes. As a result, etch pits walled with four {111} planes are formed on the {100} plane.

In the temperature region between 800°C and 1000°C, Co, Ni and Pt form a solid solution with carbon in an fcc structure [29]. The solubility of carbon into Co, Ni and Pt at 900°C estimated from the *M*-C, metal-carbon, phase diagrams is 0.8 at%, 1 at% and 0.04 at%, respectively [29]. These metal particles probably include a small amount of carbon within the limit of the solubility of respective metals. On the other hand, Fe forms in various phases with carbon at the temperature range studied between 800°C and 900°C; at 900°C for example, αFe(bcc) phase in 0~0.01 at% of carbon, αFe+γFe phase in 0.01~0.2 at% of carbon, γFe(fcc) phase in 0.2~ 5.4 at% of carbon and γFe+Fe_3C in 5.4~25 at% of carbon [29]. The reason why we assumed that Fe particles contributed to the etching of {100}HODC changed into “iron carbide” is based on the possibility of the formation of higher carbon content phases than those of Co, Ni and Pt. The Fe particles that formed a distorted round shape may be due to the fact that Fe-C binary alloy has the potential to form in various phases with different crystallographic structures within the temperature range.

5. Conclusions

The catalytic etching behavior of a highly {100}-oriented diamond coating,

{100}HODC, with hydrogen gas at temperatures between 700°C and 1000°C using Fe, Co, Ni, and Pt nanoparticles as a catalyst was examined by HRSEM and Raman spectroscopy. The metal atoms vacuum-evaporated onto the {100}HODC formed nanoparticles themselves when heated at high temperatures in a flowing gas mixture of H_2 (10%) + N_2 (90%). At 800°C, short nano-channels and etch pits holding metal nanoparticles were formed by Fe, Co, and Ni. The shapes of the Co and Ni nanoparticles in the etch pits were affected by the shape of the etch pits. The top view of the Fe nanoparticles shows a distorted round shape, probably due to the formation of something like “iron carbide”, while the carbon content is unknown. At 900°C, the etching of the {100}HODC by metal nanoparticles advanced, and vacant etch pits were also formed, while no evident etching behavior was apparently observed for the Pt-HODC except the formation of the finely dispersed platinum nanoparticles. Etching of the {100}HODC by Pt nanoparticles was clearly observed after the treatment at 1000°C for the Pt-{100}HODC. In the discussion section, the formation mechanism of the vacant etch pits and the potential etching mechanism of diamonds with hydrogen by metal nanoparticles, probably as melted metal nanoparticles, were discussed. The patterning of {100}HODCs with small etch pits holding metal nanoparticles is promising for the development of functional materials; such as agglomerate-proof metal catalysts or new electronic devices.

Acknowledgments

The highly {100}-oriented diamond coating was a gift from Kobe Steel, Ltd. We gratefully acknowledge their help.

References

[1] Y. Takasu, R. Matsuyama, S. Konishi, W. Sugimoto, Y. Murakami, Dependence of the preparation temperature of $Pt_{0.7}Co_{0.3}$/C catalysts on the structure of the alloy particles and the carbon supports, Electrochem. Solid-State Lett. 8 (2005) B34-B37.

[2] Y. Takasu, S. Konishi, R. Miyoshi, K. Nukii, T. Matsuse, W. Sugimoto, et al., Catalytic linear grooving of graphite surface layers by Pt, Ru, and PtRu nanoparticles, Chem. Lett. 34 (2005) 1008-1009.

[3] S. Konishi, W. Sugimoto, Y. Murakami, Y. Takasu, Catalytic creation of channels in

the surface layers of highly oriented pyrolytic graphite by cobalt nanoparticles, Carbon 44 (2006) 2338-2340.

[4] T. Iwazaki, T. Semba, S. Konishi, T. Sezai, Y. Murakami, W. Sugimoto, et al., Catalytic excavation and graphitization of activated carbon by cobalt nanoparticles, Chem. Lett. 37 (2008) 1194-1195.

[5] S. Konishi, T. Ohashi, W. Sugimoto, Y. Takasu, Effect of the crystal plane on the catalytic etching behavior of diamond crystallites by cobalt nanoparticles, Chem. Lett. 35 (2006) 1216-1217.

[6] Y. Takasu, S. Konishi, W. Sugimoto, Y. Murakami, Catalytic formation of nanochannels in the surface layers of diamonds by metal nanoparticles, Electrochem. Solid-State Lett. 9 (2006) C114-C117.

[7] T. Ohashi, W. Sugimoto, Y. Takasu, Catalytic roughening of surface layers of BDD for various applications, Electrochim. Acta 54 (2009) 5223-5229.

[8] D.D. Eley, P.W. Selwood, P.B. Weisz, Advances in catalysis XI, Academic Press Inc, New York and London, 1959.

[9] N. R. Khalili, M. Campbell, G. Sandi, J. Golas, Production of micro- and mesoporous activated carbon from paper mill sludge - I. Effect of zinc chloride activation, Carbon 38 (2000) 1905-1915.

[10] A. Ahmadpour, D.D. Do, The preparation of active carbons from coal by chemical and physical activation, Carbon 34 (1996) 471-479.

[11] F. Rodriguezreinoso, M. Molinasabio, M.T. Gonzalez, The use of steam and CO_2 as activating agents in the preparation of activated carbons, Carbon 33 (1995) 15-23.

[12] R.T.K. Baker, In situ electron microscopy studies of catalyst particle behavior, Catal. Rev.-Sci. Eng. 19 (1979) 161-209.

[13] Y. Tamai, H. Watanabe, A. Tomita, Catalytic gasification of carbon with steam, carbon dioxide and hydrogen, Carbon 15 (1977) 103-106.

[14] S. Jin, J.E. Graebner, M. McCormack, T.H. Tiefel, A. Katz, W.C. Dautremontsmith, Shaping of diamond films by etching with molten rare-earth-metals, Nature 362 (1993) 822-824.

[15] M. McCormack, S. Jin, J.E. Graebner, T.H. Tiefel, G.W. Kammlott, Low temperature thinning of thick chemically vapor-deposited diamond films with a molten Ce-Ni alloy, Diamond & Relat. Mater. 3 (1994) 254-258.

[16] F.K. de Theije, E. van Veenendaal, W.J.P. van Enckevort, E. Vlieg, Oxidative etching of cleaved synthetic diamond {111} surfaces, Surf. Sci. 492 (2001) 91-105.
[17] V.G. Ralchenko, T.V. Kononenko, S.M. Pimenov, N.V. Chernenko, E.N. Loubnin, V.Y. Armeyev, et al., Catalytic interaction of Fe, Ni and Pt with diamond films: patterning applications, Diamond & Relat. Mater. 2 (1993) 904-909.
[18] H. Masuda, M. Watanabe, K. Yasui, D. Tryk, T. Rao, A. Fujishima, Fabrication of a nanostructured diamond honeycomb film, Adv. Mater. 12 (2000) 444-447.
[19] J. Enlund, J. Isberg, M. Karlsson, F. Nikolajeff, J. Olsson, D.J. Twitchen, Anisotropic dry etching of boron doped single crystal CVD diamond, Carbon 43 (2005) 1839-1842.
[20] T. Tachibana, K. Hayashi, K. Kobashi, Azimuthal rotation of diamond crystals epitaxially nucleated on silicon {001}, Appl. Phys. Lett. 68 (1996) 1491-1492.
[21] A. Ōya, S. Ōtani, Catalytic graphitization of carbons by various metals, Carbon 17 (1979) 131-137.
[22] T. Ohashi, W. Sugimoto, Y. Takasu, Self-embedment of small rectangular parallelepiped platinum particle array in etch pits on {100} planes of diamond crystallites, Bull. Chem. Soc. Jpn., (available on web (March 5, 2011); doi:10.1246/bcsj.20100330).
[23] M. C. Granger, M. Witek, J. Xu, J. Wang, M. Hupert, A. Hanks, M. D. Koppang, J. E. Butler, G. Lucazeau, M. Mermoux, J. W. Strojek, G. M. Swain, Standard electrochemical behavior of high-quality, boron-doped polycrystalline diamond thin-film electrodes, Anal. Chem., 72 (2000) 3793-3804.
[24] H. B. Martin, A. Argoitia, U. Landau, A. B. Anderson, J. C. Angus, Hydrogen and oxygen evolution on boron-doped diamond electrodes, J. Electrochem. Soc. 143 (1996) L133-L136.
[25] P. Buffat, J.P. Borel, Size effect on the melting temperature of gold particles, Phys. Rev. A 13(1976) 2287-2298.
[26] S. Iijima, Helical microtubules of graphitic carbon, Nature 354 (1991) 56-58.
[27] A M. Cassell, J.A. Raymakers, J. Kong, H.J. Dai, Large scale CVD synthesis of single-walled carbon nanotubes, J. Phys. Chem. B 103 (1999) 6484-6492.
[28] L. Randall, V. Wal, T.M. Ticich, V.E. Curtis, Substrate-support interactions in metal-catalyzed carbon nanofiber growth, Carbon 39 (2001) 2277-2289.

[29] T. B. Massalski, H. Okamoto, P. R. Subramanian, L. Kacprzak, Binary Alloy Phase Diagrams, 2nd ed., ASM International, Ohio, 1990, Vol. 1, pp.835-873.

Figure Captions

Fig. 1. SEM micrographs of the as-received highly {100}-oriented diamond coating, {100}HODC, at different magnifications.

Fig. 2. SEM micrographs of the Co-{100}HODC treated at (a); 700°C, (b); 800°C

and (c); 900°C for 2 h in a flowing gas mixture of highly pure 10%H_2 and 90%N_2. The deposited amount of Co was 5.0×10^{15} Co-atoms cm^{-2}.

Fig. 3. SEM micrographs of the Ni-{100}HODC treated at (a); 800°C for 2 h, (b); 900°C for 2 h, and (c); 900°C for 24 h in a flowing gas mixture of highly pure 10%H_2 and 90%N_2. The deposited amount of Ni was 5.0×10^{15} Ni-atoms cm^{-2}.

Fig. 4. SEM micrographs of the Fe-{100}HODC treated at (a); 800°C and (b); 900°C for 2 h in a flowing gas mixture of highly pure 10%H_2 and 90%N_2. The deposited amount of Fe was 5.3×10^{15} Fe-atoms cm^{-2}.

Fig. 5. SEM micrographs of the Pt-{100}HODC treated at (a); 900°C and (b); 1000°C for 2 h in a flowing gas mixture of highly pure 10%H_2 and 90%N_2. The deposited amount of Pt was 1.5×10^{15} Pt-atoms cm^{-2}.

Fig. 6. Raman spectra of (a) pristine {100}HODC and (b) Fe-{100}HODC, (c) Co-{100}HODC and (d) Ni-{100}HODC, which were treated at 900°C for 2 h in a flowing gas mixture of highly pure 10%H_2 and 90%N_2.

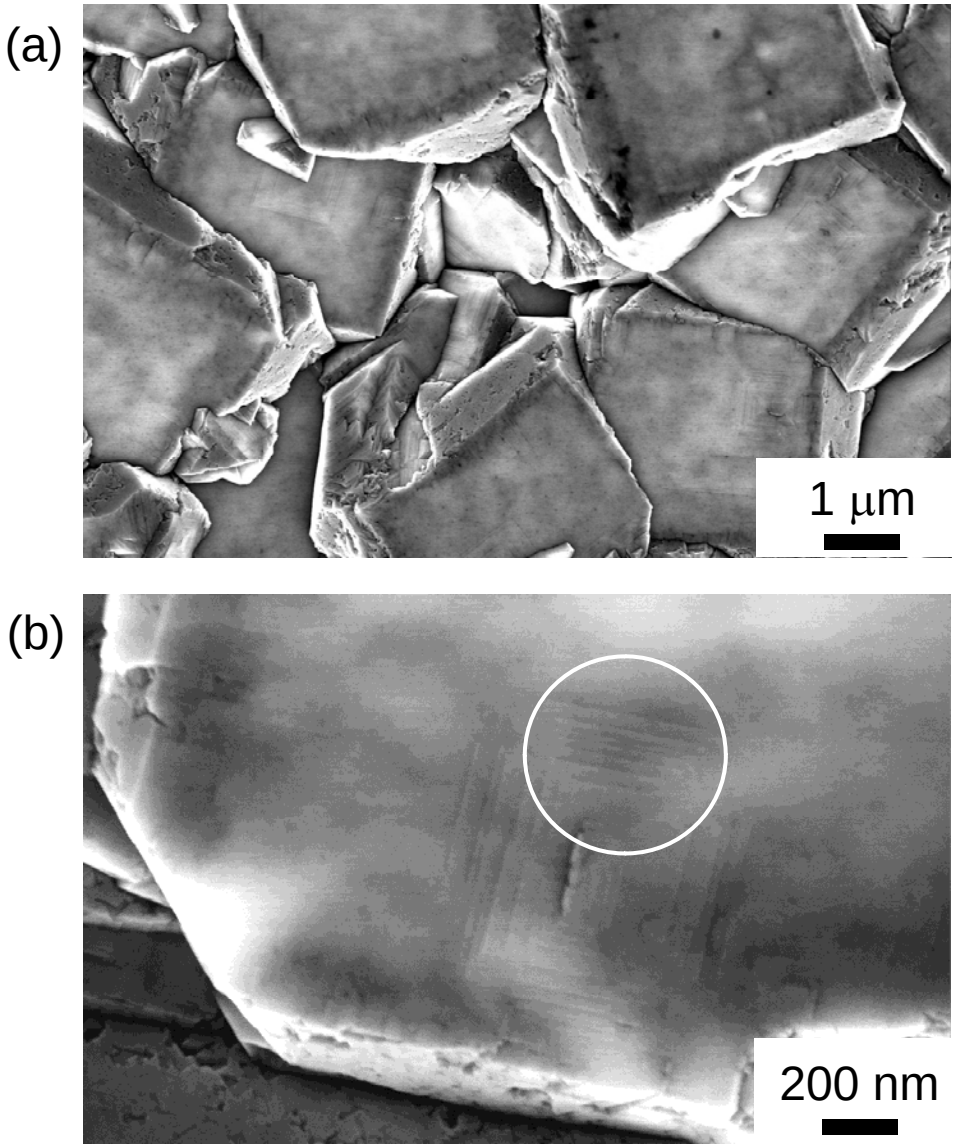

Fig. 1

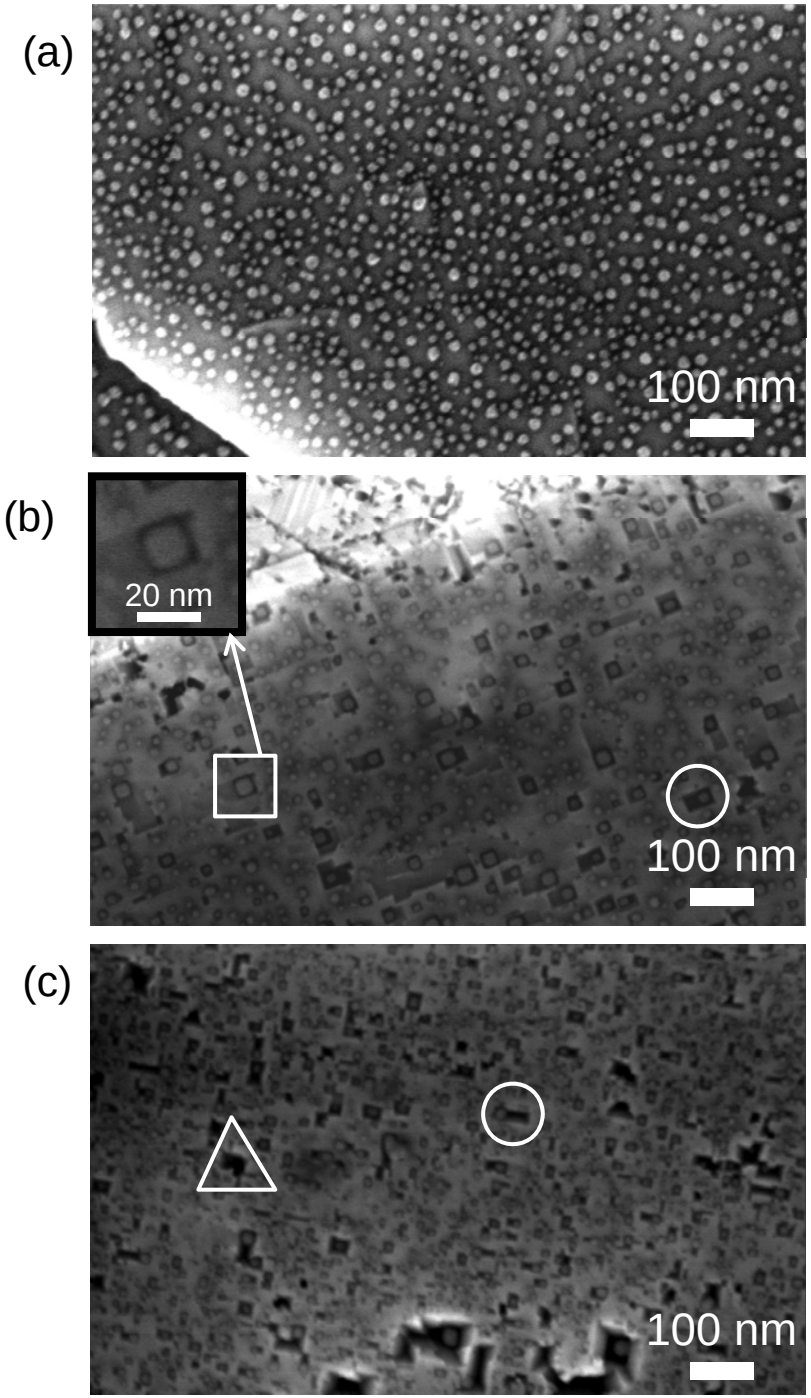

Fig. 2

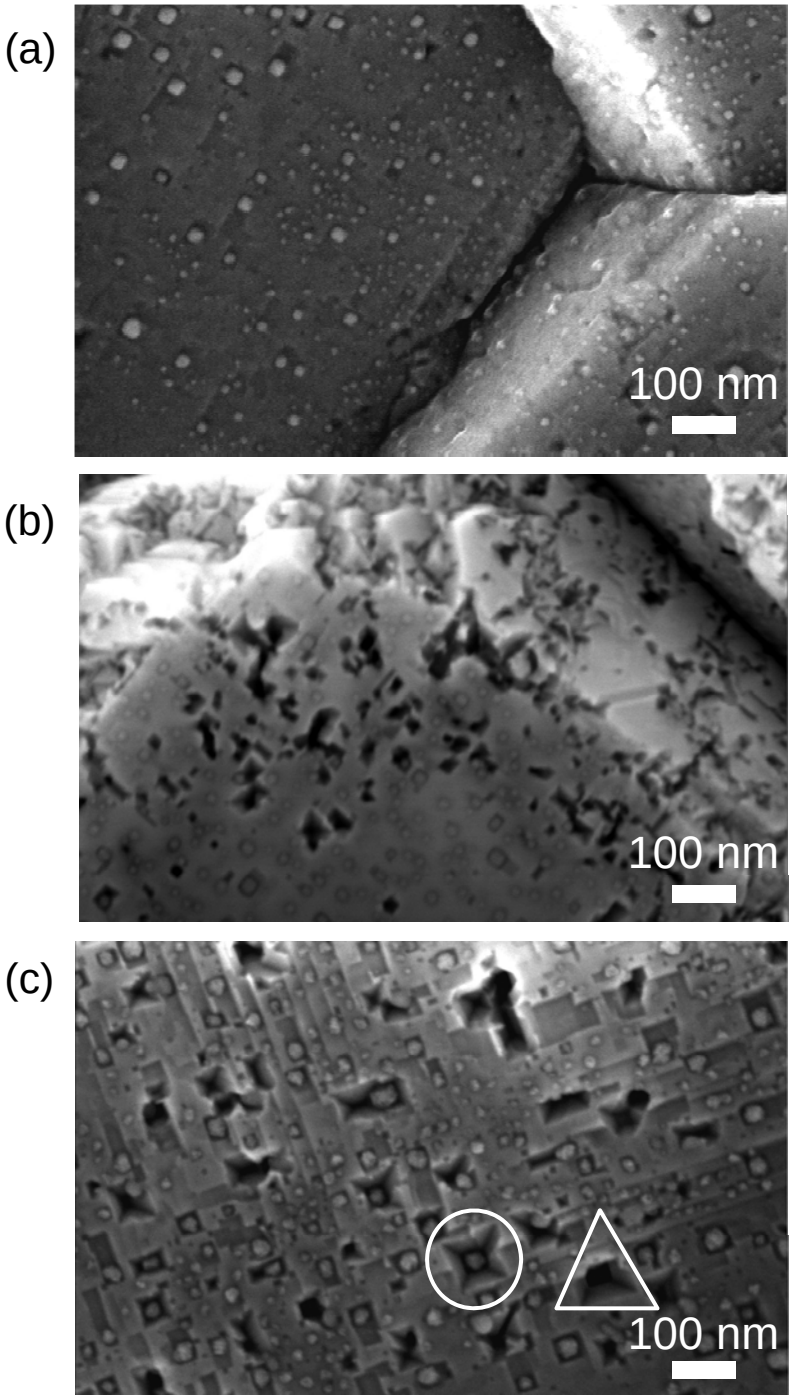

Fig. 3

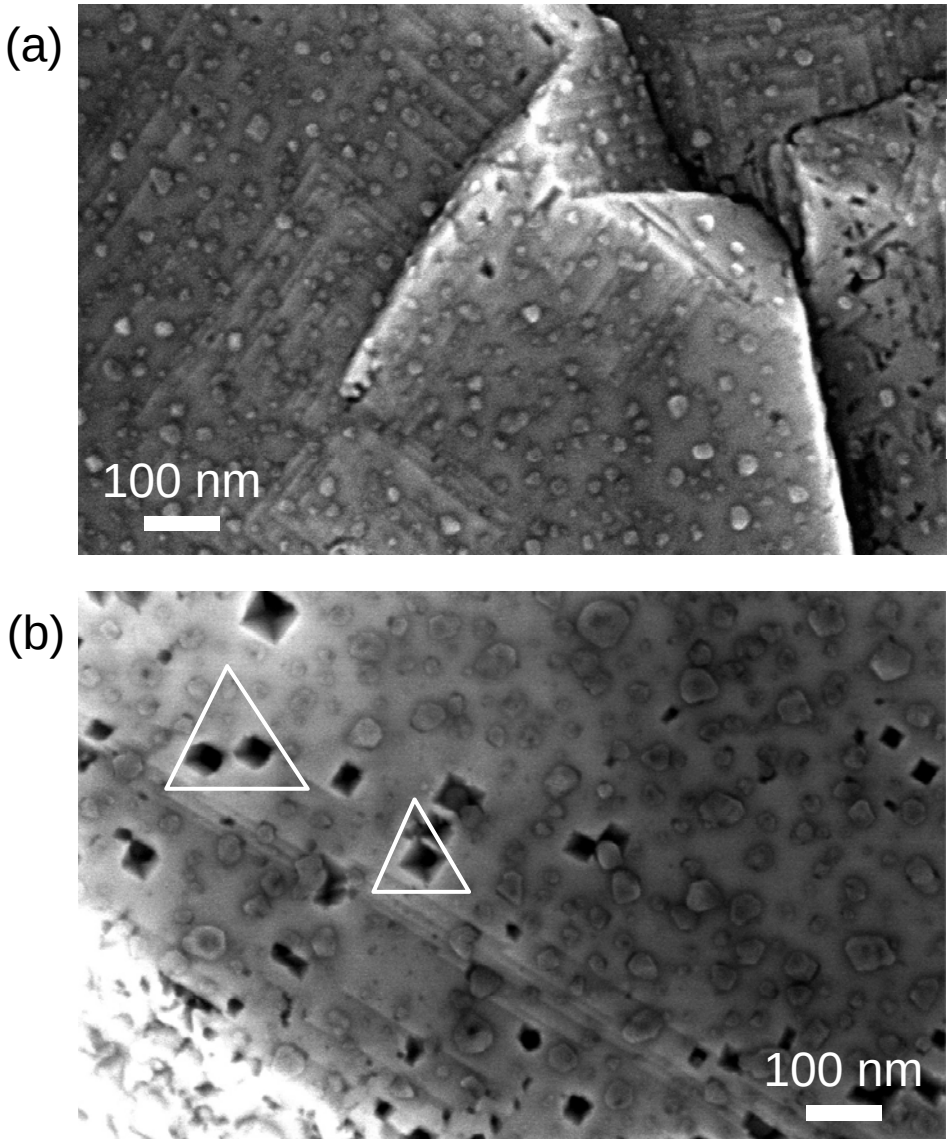

Fig. 4

(a)

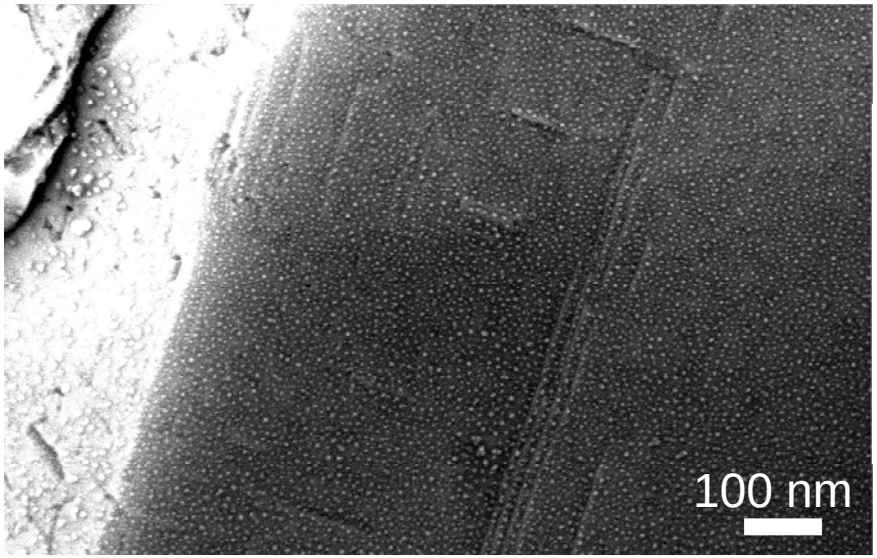

(b)

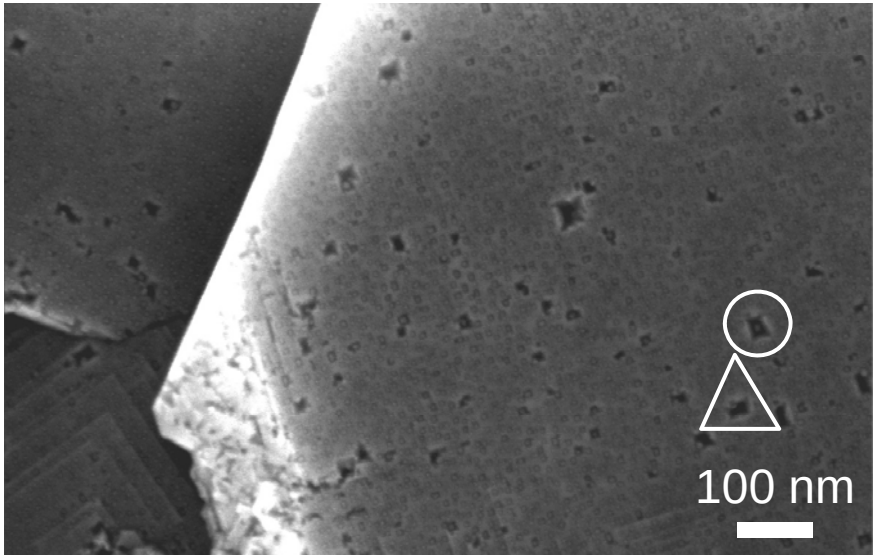

Fig. 5

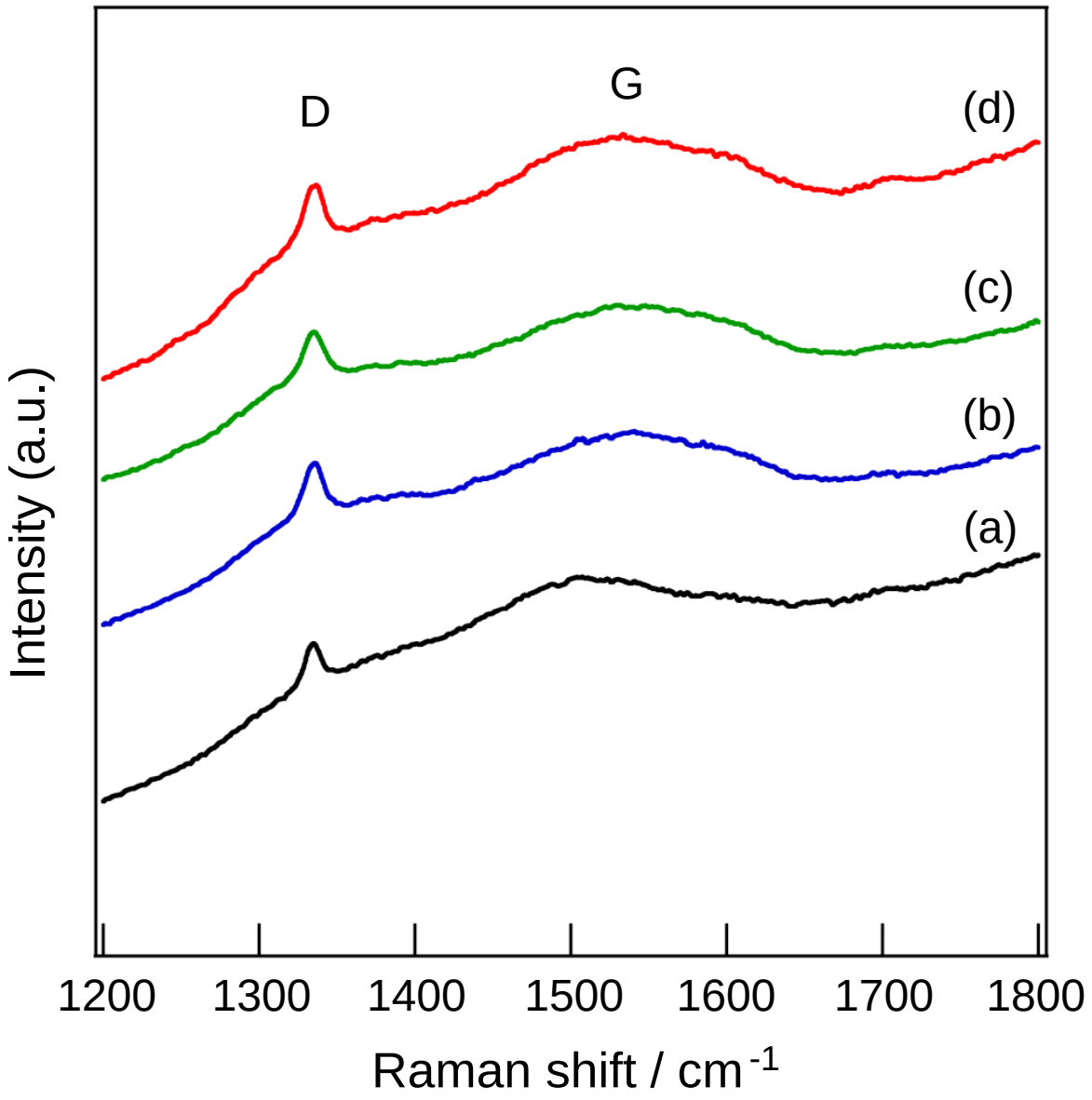
D
G
(d)
(c)
(b)
(a)
Intensity (a.u.)
1200
1300
1400
1500
1600
1700
1800
Raman shift / cm -1

Fig. 6